

Spin spiral ground state of γ -iron

K. Knöpfle, L. M. Sandratskii, and J. Kübler

Institut für Festkörperphysik, Technische Universität, D-64289 Darmstadt, Germany

(Received 15 March 2000)

Using density-functional theory we calculate the magnetic ground-state properties of γ -Fe for a large set of spiral vectors and lattice constants. The effective single-particle equations are solved by means of an advanced version of the augmented spherical waves method which takes into account the full-shape potential and the intra-atomic noncollinearity of the magnetization. Together with the generalized gradient approximation the experimentally determined spiral magnetic ground state is reproduced successfully. Symmetry properties of the intra-atomic noncollinearity of the magnetization are analyzed and illustrated for spiral magnetic structures. We conclude that γ -Fe is an itinerant electron system possessing well-defined atomic moments.

I. INTRODUCTION

Since the appearance of the experimental work of Tsunoda¹ and Tsunoda *et al.*² the spiral magnetic ground state of γ -Fe has attracted a great deal of theoretical attention. Very recent publications on this topic³⁻⁷ show that the interest is still unbroken.

γ -Fe is the fcc phase of iron which is stable at temperatures above the magnetic phase transition. At low temperatures γ -Fe can be stabilized in the form of small clusters in a Cu matrix. The magnetic structure of the clusters was found to be a spin spiral^{1,2} with a spiral vector varying from $\mathbf{q} = (0,1,0,1)$ for pure γ -Fe to $\mathbf{q} = (0.13,0,1)$ for γ -Fe_{100-x}Co_x with $x=4$ (where \mathbf{q} is given in units of $2\pi/a$).

The generalization of the methods of density-functional theory to cases of incommensurate spin spiral structures was suggested in Ref. 8. These structures were shown to become manageable because of their special symmetry properties. Subsequently, numerous first-principles calculations of the total energy of γ -Fe as a function of the spiral vector \mathbf{q} were reported.^{3-7,9-12} All calculations confirmed the spiral character of the ground state in γ -Fe but did not succeed in reproducing the experimental \mathbf{q} value. Initial studies⁹⁻¹¹ based on the local-density approximation found the minimum of the total energy at $\mathbf{q} = (0,0,0.6)$. In calculations¹² that employ the generalized gradient approximation¹³ (GGA) one finds that a minimum of the total energy remains at $\mathbf{q} = (0,0,0.6)$. The results depend, however, on the value of the lattice constant. If it is varied over some range of values another minimum emerges at $\mathbf{q} = (0.5,0,1)$ which, unfortunately, also differs from the experimental value. Bylander and Kleinman⁴⁻⁷ used a full-potential scheme, the GGA, and at last a ‘‘spin stiffness correction,’’ allowing for *intra-atomic* noncollinearity of the magnetization, but concluded that the theoretical tools were insufficiently accurate to yield the experimental value of \mathbf{q} . Thus, clearly, the correct description of the ground state of γ -Fe becomes a challenge for density-functional theory in applications to the 3d metals.

In the present paper we apply an advanced version of the augmented spherical waves (ASW) method, called modified ASW (MASW), to the analysis of this problem. The MASW method, besides using the full-shape potential inside the

atomic spheres, takes into account intra-atomic noncollinearity of the magnetization. Furthermore, the generalized gradient approximation¹³ (GGA) is employed in the calculations. In contrast to Bylander and Kleinman who restricted their calculations to the lattice constant of Cu, we extend our calculations to lattice parameters ranging from $a = 6.7a_0$ to $a = 6.95a_0$. This interval includes the lattice constant for γ -Fe, $a = 6.76a_0$, and fcc-Cu, $a = 6.822a_0$. (a_0 is the Bohr radius.)

To study the properties of the intra-atomic magnetization we analyze the symmetry of the spiral structures in terms of the generalized spin-space groups and verify that the z component of the magnetization must vanish at any point in space, the property used in the calculations of Bylander and Kleinman.

The paper is organized as follows. The MASW method is described briefly in Sec. II and is followed by an analysis of the symmetry properties of the spiral magnetic structures at hand in Sec. III. In Sec. IV the results of the calculations of the spiral magnetic states in γ -Fe are presented and discussed. We close with brief conclusions.

II. CALCULATIONAL APPROACH

Throughout the calculations the MASW method is used which, in contrast to the standard augmented spherical waves^{10,11} method, employs the full-shape potential inside the atomic spheres. Since this is standard in all full-potential methods it need not be discussed here any further. It suffices to say that an expansion in spherical harmonics to order $l = 6$ is used for the potential in the case of iron. Not yet standard is another important improvement: the standard ASW method assigns to each atomic sphere a spin-quantization axis neglecting the off-diagonal elements of the potential matrix in this local frame. In contrast to this the MASW method accounts for the noncollinearity of the *intra-atomic* magnetization by determining the full 2×2 potential matrix for each point inside the atomic spheres. Pioneering work on intra-atomic noncollinearity has been done by Nordström and Singh,¹⁴ followed by the work of other authors as, for instance, Refs. 4–7,15,16. We here limit ourselves to a short description of the potential matrix in the MASW method.

In noncollinear magnetic systems the spin projection on a

single axis is not a good quantum number. The wave functions are spinors and the density matrix is given by

$$\rho(\mathbf{r}) = \sum_{nk} \psi_{nk}(\mathbf{r}) \psi_{nk}^\dagger(\mathbf{r}). \quad (1)$$

This matrix can be diagonalized at each point \mathbf{r} in space with the help of the spin- $\frac{1}{2}$ -rotation matrices $\mathbf{U}(\mathbf{r})$. To formulate the GGA, gradients and higher derivatives of the spin-density matrix are calculated at a given point \mathbf{r} resulting in derivative matrices which are transformed by the same matrix $\mathbf{U}(\mathbf{r})$ into the local spin-coordinate system where the density matrix is diagonal. Then the diagonal elements of the density and derivative matrices are treated as usual in the GGA formalism to obtain the diagonal potential matrix in the local coordinate frame. Next, the matrix $\mathbf{U}(\mathbf{r})$ is used to transform the potential back to the global system:

$$\begin{aligned} \rho(\mathbf{r}) &= \begin{pmatrix} \rho_{\uparrow\uparrow}(\mathbf{r}) & \rho_{\uparrow\downarrow}(\mathbf{r}) \\ \rho_{\downarrow\uparrow}(\mathbf{r}) & \rho_{\downarrow\downarrow}(\mathbf{r}) \end{pmatrix} = \mathbf{U}^\dagger(\mathbf{r}) \begin{pmatrix} \rho_{\uparrow\uparrow}^{\text{loc}}(\mathbf{r}) & 0 \\ 0 & \rho_{\downarrow\downarrow}^{\text{loc}}(\mathbf{r}) \end{pmatrix} \mathbf{U}(\mathbf{r}) \\ &\rightarrow \mathbf{U}^\dagger(\mathbf{r}) \begin{pmatrix} v_{\uparrow\uparrow}^{\text{loc}}(\mathbf{r}) & 0 \\ 0 & v_{\downarrow\downarrow}^{\text{loc}}(\mathbf{r}) \end{pmatrix} \mathbf{U}(\mathbf{r}) \\ &= \begin{pmatrix} v_{\uparrow\uparrow}(\mathbf{r}) & v_{\uparrow\downarrow}(\mathbf{r}) \\ v_{\downarrow\uparrow}(\mathbf{r}) & v_{\downarrow\downarrow}(\mathbf{r}) \end{pmatrix} = \mathbf{v}(\mathbf{r}). \end{aligned} \quad (2)$$

The full spatial dependence of all quantities inside the atomic spheres is preserved in the MASW method in contrast to the standard ASW. More details of the MASW method can be found in another paper by these authors.¹⁷

III. SYMMETRY OF THE CRYSTAL AND MAGNETIC STRUCTURE

The symmetry group of a magnetic crystal is determined by both the atomic positions and the directions of the atomic moments. As in all earlier theoretical studies^{3-7,9-12} we focus on spiral structures with atomic moments within the xy plane defined by the vectors

$$\hat{\mathbf{e}}_i = (\cos(\mathbf{q} \cdot \mathbf{a}_i), \sin(\mathbf{q} \cdot \mathbf{a}_i), 0), \quad (3)$$

where $\hat{\mathbf{e}}_i$ is the direction of the spin of the atom at the position \mathbf{a}_i and \mathbf{q} is the spiral vector.

The symmetry of these spiral structures imposes restrictions on the shape of the intra-atomic charge density, magnetization, and potentials. The knowledge of these restrictions is helpful in developing efficient calculational schemes and also in analyzing the calculated data.

The symmetry of the spiral structures is described by the spin-space groups⁸ which, in contrast to the usual space groups, allow different transformations of spin and space variables. The operators of the spin space groups have the form $\{\alpha_S | \alpha_R | \mathbf{t}\}$, where α_S is a spin rotation, α_R is a space rotation, and \mathbf{t} is a space translation. By rotations we understand here the pure rotations and rotations combined with inversion. The operators are defined by

$$\{\alpha_S | \alpha_R | \mathbf{t}\} \mathbf{m}(\mathbf{r}) = \alpha_S \mathbf{m}(\{\alpha_R | \mathbf{t}\}^{-1} \mathbf{r}) = \alpha_S \mathbf{m}(\alpha_R^{-1}(\mathbf{r} - \mathbf{t})), \quad (4)$$

TABLE I. Symmetry operations of different spiral magnetic structures in γ -Fe.

	$\mathbf{q} = 2\pi/a(0,0,\gamma)$			$\mathbf{q} = 2\pi/a(\alpha,0,1)$	
E	C_{2z}	$\mathbf{U}_{2x}C_{2x}$	$\mathbf{U}_{2x}C_{2y}$	E	$\mathbf{U}_{2x}I$
C_{4z}^-	C_{4z}^+	$\mathbf{U}_{2x}C_{2b}$	$\mathbf{U}_{2x}C_{2a}$	σ_y	$\mathbf{U}_{2x}C_{2y}$
σ_x	σ_y	$\mathbf{U}_{2x}I$	$\mathbf{U}_{2x}\sigma_z$		
σ_{db}	σ_{da}	$\mathbf{U}_{2x}S_{4z}^-$	$\mathbf{U}_{2x}S_{4z}^+$		

where $\mathbf{m}(\mathbf{r})$ is the intra-atomic magnetization at point \mathbf{r} . Since the magnetization is invariant with respect to the symmetry transformation $\{\alpha_S | \alpha_R | \mathbf{t}\}$ it satisfies the following relation:

$$\mathbf{m}_i(\alpha_R \mathbf{r}_i) = \alpha_S \mathbf{m}_j(\mathbf{r}_j), \quad (5)$$

where $\mathbf{m}_i(\mathbf{r}_i)$ is the magnetization inside the atomic sphere of atom i and the vector \mathbf{r}_i is measured from the center of the sphere. The atoms i and j are connected by the space transformation

$$\{\alpha_R | \mathbf{t}\} \mathbf{a}_i = \alpha_R \mathbf{a}_i + \mathbf{t} = \mathbf{a}_j. \quad (6)$$

If $i = j$ and $\alpha_R \mathbf{r}_i = \mathbf{r}_i$ in Eq. (5) we obtain a restriction on the magnetization at the given point \mathbf{r}_i otherwise a relation of the magnetization at two different points is obtained.

The symmetry properties of spiral structures are discussed in detail in Ref. 18. In Table I we collect the symmetry operations for the spiral structures studied in this paper. The operations shown do not include space translations. The operations C_2 are space rotations by π , C_4 are rotations by $\pm \pi/2$, σ are space reflections, I is the inversion, and S_4 are rotation reflections; \mathbf{U}_{2x} are spin rotations about the x axis by π . For some operations the spin transformation is unity and is omitted in the notation.

At the points on symmetry lines and planes, the operations collected in Table I impose restrictions on the values of the components of the magnetization. For example, operation $\mathbf{U}_{2x}\sigma_z$ leaves all points with $z=0$ invariant and transforms the magnetization as $\mathbf{U}_{2x}(m_x(\mathbf{r}), m_y(\mathbf{r}), m_z(\mathbf{r})) = (m_x(\mathbf{r}), -m_y(\mathbf{r}), -m_z(\mathbf{r}))$. Therefore, at each point in the plane $z=0$, $m_y(\mathbf{r})$, and $m_z(\mathbf{r})$ must be zero. For a general point in the atomic sphere, symmetry determines the relative direction of magnetization with respect to the magnetization at equivalent points. For example, the symmetry operation $\mathbf{U}_{2x}I$ leads to the relation $(m_x(\mathbf{r}), m_y(\mathbf{r}), m_z(\mathbf{r})) = (m_x(-\mathbf{r}), -m_y(-\mathbf{r}), -m_z(-\mathbf{r}))$ at points \mathbf{r} and $-\mathbf{r}$.

Further information on the properties of the magnetization can be obtained by taking into account the time-reversal operation. Although the time reversal itself cannot be a symmetry operation of a magnetic crystal, the combination of time reversal with an appropriate operation $\{\alpha_S | \alpha_R | \mathbf{t}\}$ might leave a magnetic crystal invariant. Indeed, in our case there is an additional symmetry operation $\mathbf{U}_{2z}\Theta$ leaving the spiral structures under consideration invariant. Here Θ is the time-reversal operation. Since this operation does not act on the space variable it leads to a symmetry restriction on the magnetization at each point \mathbf{r} : $(m_x(\mathbf{r}), m_y(\mathbf{r}), m_z(\mathbf{r})) = (m_x(\mathbf{r}), m_y(\mathbf{r}), -m_z(\mathbf{r}))$. As a result $m_z(\mathbf{r})=0$ at each point \mathbf{r} . Note that operations of the kind $\mathbf{U}_{2z}\Theta$ can be symmetry operations of the physical problem only if spin-orbit

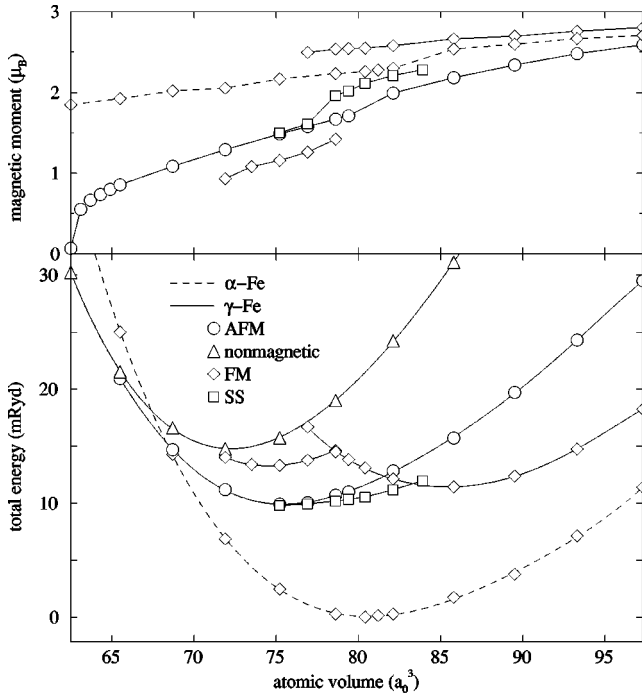


FIG. 1. Magnetic moments (top) and total energies (bottom) calculated with the MASW method using the GGA for ferromagnetic (FM), antiferromagnetic (AFM), nonmagnetic, and spiral structures (SS) in cubic (α and γ) iron as a function of atomic volume.

coupling can be neglected. Otherwise the spin and space variables are coupled and must be transformed in the same way.

IV. CALCULATIONAL RESULTS

A. Spiral magnetic states in γ -iron

To test the reliability of our new calculational technique and to locate the spin spiral states in the magnetic phase diagram of cubic iron we carried out calculations of various states of α -Fe (bcc-Fe) and γ -Fe for a broad range of lattice parameters. A selection of our results is shown in Fig. 1, where, comparing the two structures, we graph the total energy as a function of atomic volume. The seven data points labeled SS in Fig. 1 are minimum-energy spiral ground states corresponding to the following lattice constants: $a = 6.7a_0$, $6.75a_0$, $6.8a_0$, $6.822a_0$, $6.85a_0$, $6.9a_0$, and $6.95a_0$.

The calculations reproduce all important features of the phase diagram of cubic Fe: in agreement with experiment the ground state of iron is a ferromagnetic bcc structure. For the fcc structure we obtain two ferromagnetic phases, a low-moment phase at smaller volumes and a high-moment phase at larger volumes. The high-moment phase has lower energy. But the antiferromagnetic phase of fcc iron has an even lower total energy at small volumes, crossing the ferromagnetic state at a higher volume. In the vicinity of this crossover the spiral state possesses the lowest total energy. The equilibrium lattice constant of $a = 5.44a_0$ and the calculated magnetic moment of $2.26\mu_B$ of the bcc ground state are in excellent agreement with the experimental values $a = 5.42a_0$ (Ref. 19) and $2.23\mu_B$.²⁰

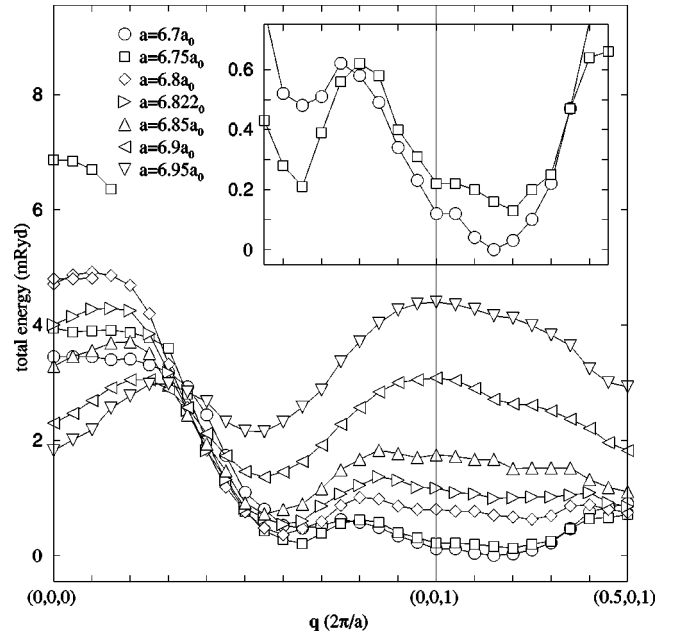


FIG. 2. The total energy $E_{\text{tot}}(\mathbf{q})$ of γ -Fe for \mathbf{q} along two directions in the Brillouin zone and for different lattice constants.

Turning now to a detailed discussion of the spiral magnetic states we show the \mathbf{q} dependence of the total energy in Fig. 2. These calculations were carried out for planar spirals characterized by the polar angle $\theta = \pi/2$ and the vectors $\mathbf{q} = (0,0,\gamma)$ with $0 \leq \gamma \leq 1$ and $\mathbf{q} = (\alpha,0,1)$ with $0 \leq \alpha \leq 0.5$. For the range of lattice constants $a = 6.7a_0$ to $a = 6.9a_0$, the spiral structures provide the states having total energies lower than the collinear states, those of minimal energy being shown in Fig. 1.

We see that the form of the total-energy curves changes drastically with variation of the lattice parameter. For $a = 6.95a_0$ the minimum of the total energy corresponds to the ferromagnetic state $\mathbf{q} = (0,0,0)$. Furthermore, there are two local minima at $\mathbf{q} \approx (0,0,0.5)$ and $\mathbf{q} = (0.5,0,1)$. For $a = 6.9a_0$ down to $a = 6.8a_0$ the minimal energy corresponds to the spiral with $\mathbf{q} \approx (0,0,0.55)$. This state was discussed in most of the earlier calculations. At $a = 6.75a_0$ and $a = 6.8a_0$ near $\mathbf{q} = (0,0,0)$ a high-moment and a low-moment phase coexist (compare with Fig. 1).

For $a \leq 6.75a_0$ we observe the formation of a new total-energy minimum at $\mathbf{q} \approx (0.15,0,1)$. This \mathbf{q} value is in perfect agreement with the experimental value reported. The inset in Fig. 2 exposes the details of $E(\mathbf{q})$ in the region of this minimum. At $a = 6.75a_0$ the minimum near the experimental \mathbf{q} value is slightly lower than at $\mathbf{q} = (0,0,0.65)$. The trend becomes much clearer for $a = 6.7a_0$.

Bylander and Kleinman^{4,6} used only the lattice constant of Cu ($a = 6.822a_0$) for their calculations; this may be the reason why they did not obtain the total-energy minimum at the experimental spiral vector. For this lattice constant we obtain in agreement with their results^{4,6} a total-energy minimum at $\mathbf{q} = (0,0,0.6)$. Our calculations show that the relaxation of the bulk of the precipitates to lower lattice parameters characteristic for γ -Fe can be essential for the formation of the spiral structure with the experimentally determined \mathbf{q} . This relaxation of the lattice constant is observed in γ -Fe epitaxially grown on Cu. For layers with more than 5 monolayers Fe the

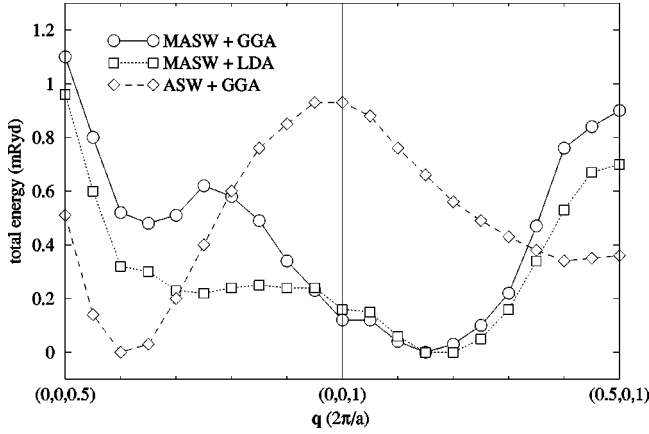


FIG. 3. Spiral magnetic states calculated with different schemes.

lattice constant relaxes from the Cu value in the first two layers to the lattice constant of γ -Fe ($a = 6.76a_0$) in the interior.²¹

We now reveal the physical interactions responsible for the formation of the total-energy minimum at the experimental \mathbf{q} value. For this purpose we carry out a number of calculations of $E(\mathbf{q})$ for $a = 6.7a_0$ using different approximations. In Fig. 3 we compare the $E(\mathbf{q})$ curves calculated with three different approaches: our standard calculation scheme (MASW+GGA), the MASW method without gradient correction (MASW+LDA) and the standard ASW with gradient correction (ASW+GGA). The ASW+GGA results clearly show that the gradient correction alone cannot improve the standard ASW calculation. The decisive changes come about through either the full-potential calculations or the intra-atomic noncollinearity or both since these are the features that distinguish MASW from the standard ASW method. In fact, except for a slight shift, the gradient correction in the MASW calculations leads to only moderate changes of $E(\mathbf{q})$ near the experimental \mathbf{q} . However, since there is a strong change of $E(\mathbf{q})$ for other values of \mathbf{q} the gradient correction must be considered important for the description of the magnetic properties of γ -Fe.

Having thus established the importance of intra-atomic noncollinearity and the full potential for a correct description of the magnetic ground state of γ -Fe, it is natural to ask, which of these two effects is dominant. To attempt an answer the total energy is calculated by constraining the magnetization to be collinear inside the atomic spheres. In Fig. 4 the results of the constrained MASW calculation are compared with those of the unconstrained MASW calculation. For the collinear structures with $\mathbf{q} = (0,0,0)$ and $\mathbf{q} = (0,0,1)$ both calculations give identical results since the intra-atomic magnetization is collinear. For structures with strong *interatomic* noncollinearity, e.g., for $\mathbf{q} = (0,0,0.6)$, the difference of the total energies for the two calculations increases up to 0.3 mRyd. There is also a noticeable shift of the position of the total energy minima (see insert in Fig. 4). Since the intra-atomic noncollinearity is important we next discuss its properties in detail.

B. Intra-atomic magnetization

This section is devoted to the properties of the intra-atomic spin density, in particular to the noncollinearity of the

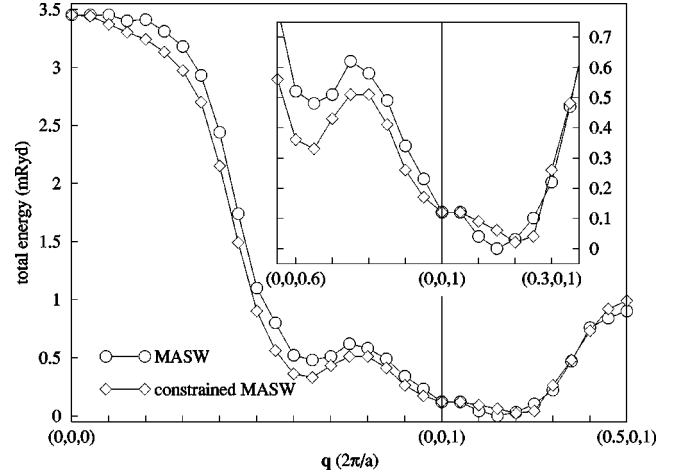


FIG. 4. Total-energy spectra $E(\mathbf{q})$ calculated with constrained and unconstrained intra-atomic magnetization.

intra-atomic magnetization. In the previous section we have shown a noticeable influence of the intra-atomic noncollinearity on the form of the $E(\mathbf{q})$ curve. On the other hand, the change of the total energy resulting from the intra-atomic noncollinearity is much smaller than the scale of the total energy change connected with the interatomic noncollinearity. Here by taking a closer look at one selected spiral state we discuss the strength, symmetry, and spatial dependence of the deviation of the intra-atomic magnetization from the direction of the atomic moment.

To better visualize the effect we chose a spiral with $\mathbf{q} = (0,0,0.65)$ which is characterized by a strong noncollinearity of the spins of neighboring atoms. In Fig. 5 we show the in-plane magnetization for the planes with $z = 0, 1.15a_0$, and $\pm 2.1a_0$. The atomic center coincides with the coordinate origin. For the $z = 0$ plane [Fig. 5(a)] there is no deviation of the magnetization from the direction of the atomic moment. On the basis of the symmetry analysis we have shown in Sec. III that the magnetization at each point in this plane must be exactly parallel to the x axis due to the symmetry operation $U_{2x}\sigma_z$.

For the planes $z \neq 0$ there is no symmetry restriction forcing the in-plane magnetization to be collinear to the direction of the atomic moment. Indeed, inspection of the Figs. 5(b)–5(d) shows noticeable deviations of the magnetization from the x axis. Vectors of the magnetization at different points of the same cross section are not exactly collinear. From Figs. 5(b)–5(d) it is clearly seen that each cross section with $z \neq 0$ supplies a nonzero contribution to the y component of the atomic moment. Thus for the plane at $z = 2.1a_0$ the contribution is negative and for the plane at $z = -2.1a_0$ it is positive. We can, however, show that these contributions compensate and the atomic magnetic moment obtained by integration over the whole atomic sphere possesses zero projection on the y axis. This property is a consequence of the symmetry operations which transform the points of the plane $z = d$ to the points of the plane $z = -d$ and the corresponding magnetization from $(m_x, m_y, 0)$ to $(m_x, -m_y, 0)$. This property is illustrated in Figs. 5(c) and 5(d).

To characterize the intra-atomic noncollinearity quantitatively we show in Fig. 6 the angle $\phi(\mathbf{r})$ between the magnetization and the direction of the atomic moment at the points

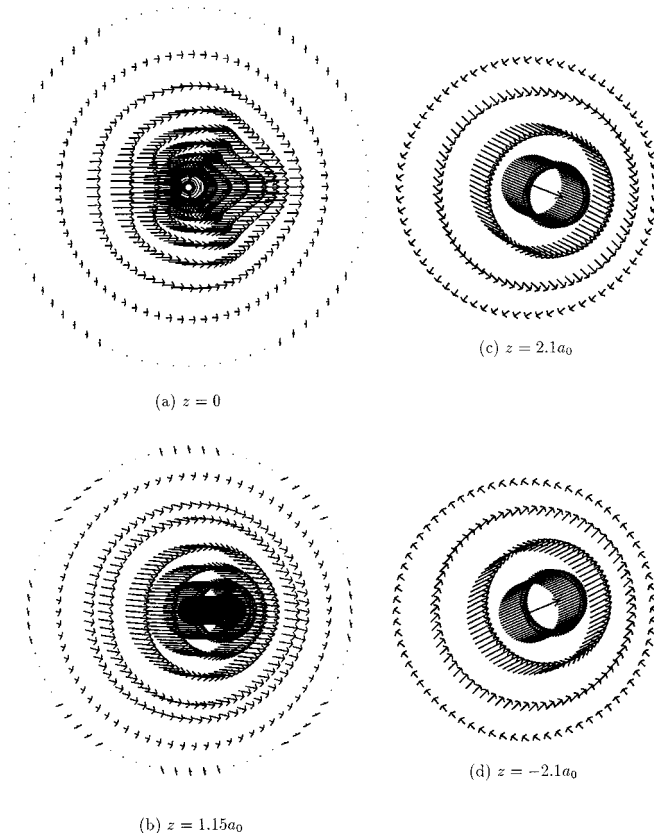


FIG. 5. Magnetization in several xy planes. The arrows are plotted enlarged by a factor 3 in (b) compared to (a) and by a factor 6 in (c) and (d).

of the (101) axis. The (101) axis connects two nearest atoms of the fcc lattice. For the spiral structure used in the calculation the angle between the atomic moments of the two neighboring atoms is equal to 117° . Figure 6 shows that in spite of a large interatomic angle the intra-atomic noncollinearity within the atom increases only slowly. The leading variation of the magnetization direction occurs at the border of the atomic sphere where the magnetic density is small. In the spatial region where the $3d$ states have a large probability amplitude, determining the value and direction of the atomic magnetic moment, the deviation of the intra-atomic magnetization from the direction of the atomic moment is small compared to the interatomic angle. This result allows us to draw the conclusion that in the case of γ -Fe we deal with a well-defined atomic moment formed by the itinerant $3d$ electrons. It would be of interest to carry out similar calculations in the case of nickel where the atomic moment is much smaller and a stronger variation of the direction of the magnetization within an atomic sphere can be expected.

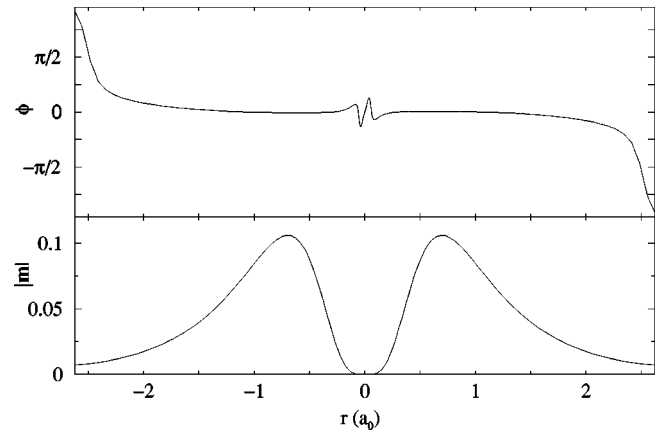


FIG. 6. Angle ϕ between magnetization direction and x axis and length of magnetization $|\mathbf{m}(\mathbf{r})|$. Vector \mathbf{r} varies along the (101) direction.

The form of our curve $\phi(\mathbf{r})$ is in good agreement with the results of Bylander and Kleinman.⁴ In addition, we relate the variation of the magnetization direction to the value of the magnetization.

V. CONCLUSIONS

An advanced version of the ASW method is used for an extensive study of the magnetic properties of γ -Fe. This version takes into account the full-shape potential inside the atomic spheres and the noncollinearity of the magnetization on an intra-atomic scale. The spatial variation of the densities is taken into account by using the GGA. We succeeded in describing the magnetic ground state of γ -Fe. The equilibrium spiral vector $\mathbf{q}=(0.15,0,1)$ obtained in the calculations is in very good agreement with the experimental value. We analyze the role of effects due to intra-atomic noncollinearity and the full potential and compare the results of LDA and GGA calculations. Symmetry properties of the intra-atomic magnetization are described and exemplarily visualized.

We show that γ -Fe has a well defined atomic moment. This means in particular that even though the magnetization is strongly noncollinear on an interatomic scale, large deviations of the magnetization from the direction of the atomic moment is seen mainly at the border of the atomic sphere where the value of the magnetic density is small.

ACKNOWLEDGMENTS

This work was supported by the Deutsche Forschungsgemeinschaft (DFG) with its SFB-Program (252) Darmstadt, Frankfurt, Mainz.

¹Y. Tsunoda, J. Phys.: Condens. Matter **1**, 10 427 (1989).

²Y. Tsunoda, Y. Nishioka, and R. M. Nicklow, J. Magn. Magn. Mater. **128**, 133 (1993).

³Y. Kakehashi and N. Kimura, Phys. Rev. B **60**, 3316 (1999).

⁴D. M. Bylander and L. Kleinman, Phys. Rev. B **58**, 9207 (1998).

⁵L. Kleinman, Phys. Rev. B **59**, 3314 (1999).

⁶D. M. Bylander and L. Kleinman, Phys. Rev. B **59**, 6278 (1999).

⁷D. M. Bylander and L. Kleinman, Phys. Rev. B **60**, 9916 (1999).

⁸L. M. Sandratskii, Phys. Status Solidi B **135**, 167 (1986).

⁹O. N. Mryasov, A. I. Liechtenstein, L. M. Sandratskii, and V. A. Gubanov, J. Phys.: Condens. Matter **3**, 7683 (1991).

¹⁰M. Uhl, L. M. Sandratskii, and J. Kübler, J. Magn. Magn. Mater.

- 103**, 314 (1992).
- ¹¹M. Uhl, L. M. Sandratskii, and J. Kübler, Phys. Rev. B **50**, 291 (1994).
- ¹²M. Körling and J. Ergon, Phys. Rev. B **54**, 8293 (1996).
- ¹³J. P. Perdew, K. Burke, and M. Ernzerhof, Phys. Rev. Lett. **77**, 3865 (1996).
- ¹⁴L. Nordström and D. J. Singh, Phys. Rev. Lett. **76**, 4420 (1996).
- ¹⁵T. Oda, A. Pasquarello, and R. Car, Phys. Rev. Lett. **80**, 3622 (1998).
- ¹⁶H. Eschrig and V. D. P. Servedio, J. Comput. Chem. **20**, 23 (1999).
- ¹⁷K. Knöpfle, L. M. Sandratskii, and J. Kübler (unpublished).
- ¹⁸L. M. Sandratskii, J. Phys.: Condens. Matter **3**, 8565 (1991); **3**, 8587 (1991).
- ¹⁹R. Kohlhaas, P. Dunner, and N. Schmitz-Pranghe, Z. Angew. Phys. **23**, 245 (1967).
- ²⁰R. Pauthenet, *Conference on High Field Magnetism* (North-Holland, Amsterdam, 1983), p. 77.
- ²¹B. Schirmer and M. Wuttig, Phys. Rev. B **60**, 12 945 (1999).